Rma56I18

NACA RM A56I18

NACA

RESEARCH MEMORANDUM

EXPERIMENTAL INVESTIGATION OF A METHOD OF WAVE-DRAG

REDUCTION FOR COMBINATIONS EMPLOYING QUASI-

CYLINDRICAL BODIES AND SWEPT WINGS AT

SUPERSONIC SPEEDS

By Daniel P. Hickey

Ames Aeronautical Laboratory
Moffett Field, Calif.

NATIONAL ADVISORY COMMITTEE
FOR AERONAUTICS
WASHINGTON
February 19, 1957

NATIONAL ADVISORY COMMITTEE FOR AERONAUTICS

RESEARCH MEMORANDUM

EXPERIMENTAL INVESTIGATION OF A METHOD OF WAVE-DRAG

REDUCTION FOR COMBINATIONS EMPLOYING QUASI-

CYLINDRICAL BODIES AND SWEPT WINGS AT

SUPERSONIC SPEEDS

By Daniel P. Hickey

SUMMARY

Axisymmetric and nonaxisymmetric body distortions designed by the method of NACA TN 3722 were tested to determine the amount of wave-drag reduction obtainable when applied to swept-wing-body combinations over a Mach number range of 1.39 to 1.97. Two wings of aspect ratios 1.33 and 2.67 were tested on different bodies. Both the axisymmetric and nonaxisymmetric distortions produced drag reductions.

INTRODUCTION

There are several theoretical methods available for reducing the wave drag of supersonic aircraft. One method, known as the supersonic area rule (ref. 1), is a slender-body theory that gives only axisymmetric body distortions. A second method is that of Nielsen (ref. 2) which is a quasi-cylindrical theory that gives additive axisymmetric and non-axisymmetric distortions. A third is the method of distributing drag-canceling multipoles along a body axis employed by Lomax and Heaslet (ref. 3). This theory, which is, in principle, exact to the order of linear theory, also gives additive axisymmetric and nonaxisymmetric distortions. Reference 2 shows that for the cases where the theories of both references 2 and 3 are applicable, the two agree to the order of quasi-cylindrical theory.

In the present investigation the primary purpose was to assess the ability of the axisymmetric and nonaxisymmetric body distortions of the quasi-cylindrical theory of reference 2 to produce drag reductions. The optimum distortion for minimum wave drag can be expressed in terms of a Fourier $\cos 2n\theta$ series. The first harmonic of distortion occurs when $n = 0$

and produces a body shape which is circular in cross section similar to the cross sections produced by transonic and supersonic area rules. The second harmonic of distortion occurs when $n = 1$ and produces a $\cos 2\theta$ variation in the body radius. The effects of the first and second harmonic terms on the body radius are additive; the first harmonic of distortion represents a volume change, while the second harmonic of distortion represents a radial redistribution of cross-sectional area. A secondary purpose of this investigation was a comparison of the drag reductions obtainable from the axisymmetric distortions produced by the quasi-cylindrical and supersonic area-rule theories.

Models using these various types of body distortions were tested in conjunction with swept wings. All the models were designed to minimize wave drag at a Mach number of $\sqrt{2}$ with a wing aspect ratio of 1.33. The bodies were tested with a wing of aspect ratio 2.67 to determine how sensitive the drag reductions were to changes in aspect ratio from the design aspect ratio. The wing-body combinations also were tested at Mach numbers of 1.75 and 1.97 to check the sensitivity of the drag reductions to changes in Mach number from the design value.

SYMBOLS

a	basic body radius, in.
A	aspect ratio, $\dfrac{4(s - a)^2}{S}$
$B_1W_1,\ldots,$ B_5W_2	wing-body combination
$\bar{c}$	mean aerodynamic chord, in.
c_d	section drag coefficient
C_D	foredrag coefficient based on plan-form area of exposed wing panels, $\dfrac{D}{qS}$
$C_{D_{W(d)}}$	wave drag of wing in combination with body due to body distortion
$C_{D_{B(d+w+i)}}$	wave drag of body in combination with wing, due to presence of body distortion, wing, and interference
ΔC_D	increment in drag due to lift, $C_D - C_{D_{min}}$
$\dfrac{\Delta C_D}{C_L{}^2}$	drag-rise factor
$C_{D_{min}}$	minimum foredrag coefficient

$\Delta C_{D_{min}}$ — change in minimum foredrag coefficient of the wing-body combinations due to the addition of the body distortion

C_L — lift coefficient based on plan-form area of exposed wing panels, $\dfrac{L}{qS}$

C_{L_α} — lift-curve slope at zero lift

C_m — pitching-moment coefficient based on plan-form area of exposed wing panels, $\dfrac{L\overline{x}}{qS\overline{c}}$

C_{m_α} — pitching-moment-curve slope at zero lift

D — foredrag, lb

L — lift, lb

$L\overline{x}$ — pitching-moment taken about centroid of exposed wing plan-form area, in-lb

M_∞ — free-stream Mach number

n — integer $0, 1, \ldots$ (used to denote harmonic of distortion)

q — free-stream dynamic pressure, lb/sq in.

r, θ — polar coordinates in y,z plane; $y = r \cos \theta$, $z = r \sin \theta$

r_B — radial distance to point on body of combination, in.

s — semispan of wing-body combination, in.

S — plan-form area of exposed wing panels, sq in.

$\dfrac{t}{c}$ — wing thickness to chord ratio

W_1, W_2 — wing-alone (exposed panels joined together)

x,y,z — coordinate axes with origin at vertex of wing alone; x measured downstream, y laterally starboard, and z vertically upward, in.

$\overline{x}$ — longitudinal distance from center of pressure of wing-body combination to centroid of wing plan-form area, in., positive when center of pressure of combination lies forward of the centroid of exposed wing plan-form area

α — angle of attack in radians unless otherwise noted

β — $\sqrt{M_\infty^2 - 1}$

δ $a - r_B$, in.

$\dfrac{\delta}{a}$ relative body distortion thickness

λ $\dfrac{1 - (r_B/a)}{\beta(t/c)}$

Subscripts

1, 2,..., 5   numbers used to identify particular components of the wing-body combinations

THEORETICAL CONSIDERATIONS

Mechanics of Body Distortions

There are several types of body distortions which reduce the wave drag of wings in combination with bodies by creating a favorable pressure field on the wings. These body distortions are actually indentations on the body which throw a negative pressure field on the forward-facing portion of the wing and a positive pressure field on the rearward-facing portion of the wing. By increasing the magnitude, δ/a, of any of these distortions, the wave-drag reduction of the wing can be increased as shown by the curve labeled $C_{D_{W(d)}}$ in sketch (a). However, by the addition of distortions to the body, the wave-drag of the body increases as shown by the curve labeled $C_{D_{B(d+w+i)}}$. The sum of the two curves, $\Delta C_{D_{min}}$, represents the wave-drag change of the wing-body combinations due to the addition of the body distortions. In general, the curve of $\Delta C_{D_{min}}$ has an optimum point as shown in the sketch. The problem of optimizing the wave drag of a wing-body combination amounts to finding the shape and magnitude of the body distortions which give the largest negative value of $\Delta C_{D_{min}}$ within the restriction of the design conditions.

Sketch (a)

In reference 2 this is done by first computing all components (including interference components) of the wave drag for a wing-body combination with arbitrary body distortions. This method requires the assumption that the body be quasi-cylindrical adjacent to the region occupied by the wing. As previously mentioned, the drag is obtained in the form of a Fourier
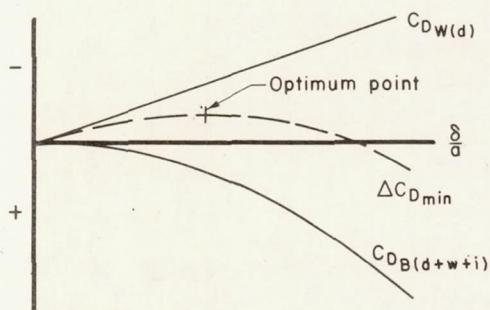
cosine series. Each term of the series for the total drag is then mini-
mized with the body distortions as the variable. It is found that the
body distortions are proportional to the magnitude of the pressures on
the wing alone. Hence, it is necessary to predict accurately the wing-
alone pressures if the body distortions are to be properly designed.
Also, since the body distortions are proportional to the wing thickness,
it is apparent that if the wing thickness were too large, the body distor-
tions would be excessive and would therefore violate the assumption of a
quasi-cylindrical body.

Effect of Mach Number

Theoretically, the body distortions become less effective at Mach
numbers other than that for which the distortions were optimized. The
physical reason for this effect is shown in the upper sketch of figure 1.
If the design Mach number is $\sqrt{2}$ and the wing leading and trailing edges
are swept 45° as indicated in the figure, then at the design Mach number
the Mach waves and pressure waves are parallel to the wing edges. As a
result, the drag-reducing pressure waves impinge on each section of the
wing at the same chordwise position and reduce the wave drag of each
section. As the Mach number increases, the drag-reducing pressure waves
are swept rearward and are less effective as shown by the theoretical
curves in the lower portion of figure 1. The quantity c_d is the section
drag coefficient due only to the body distortions. For a fixed value of
M_∞, the effect of the Mach wave displacement from the design position is
most severe at large values of r/a. For wing sections at large enough
values of r/a, the section drag is actually increased.

Effect of Aspect Ratio

At a fixed M_∞, there is a dependence of the drag reduction on
aspect ratio. The reason for this is associated with the Mach number
effect shown in figure 1 and discussed in the preceding section. There
it was pointed out that the displacement of the Mach waves from the
design condition had the most severe effects on the sections of the wing
at large values of r/a. Therefore, for a given chord length, low-aspect-
ratio wings are less affected by a rearward displacement of the Mach waves
than are the higher aspect ratio wings. Another effect associated with
the aspect ratio is shown by the $M = \sqrt{2}$ curves in the lower part of
figure 1. The curves show that even when the Mach waves are not displaced
from the design position, the effectiveness of the body distortions on
drag reduction diminishes as r/a increases. This is a result of the
fact that the pressure disturbances from the distorted portion of the
bodies attenuate approximately as $1/\sqrt{r}$.

EXPERIMENTAL CONSIDERATIONS

Apparatus

Wind tunnel.- The tests were performed in the Ames 1- by 3-foot
supersonic wind tunnel No. 2 which is of the blowdown type. This tunnel
has a flexible-plate nozzle which can be adjusted to produce nominal Mach
numbers from 1.4 to 3.8.

Models.- Five bodies and two wings as shown in figure 2 were con-
structed of steel. Table 1 presents the necessary information to deter-
mine the ordinates of the distorted bodies. Body 1 is a cone-cylinder
to which no distortion has been applied; bodies 2, 3, and 4 have the
cylindrical portion modified according to the quasi-cylindrical theory
of reference 2 (see equations in table I); body 2 has the axisymmetric
$n = 0$ distortion; and body 4 has the combined $n = 0$ and $n = 1$ distortion.
As will be discussed later, the $n = 1$ distortion of body 4 was found to
be too large due to an inadequacy of linear theory for sonic-leading-edge
wings. For this reason, body 3 was constructed with the $n = 0$ distortion
and only half the $n = 1$ distortion. Body 5 has the axisymmetric distor-
tion given by the supersonic area rule. It should be noted at this point
that the afterbodies of the combinations tested were not altered in
accordance with the theories which were used to design the models; the
body cross sections remain the same from the root of the wing trailing
edge to the base of the models. From theoretical analysis, it was found
that for the models tested, the drag reductions additionally obtained
from fairing the afterbody would be negligible. For the purpose of this
report, the distortions are referred to as the quasi-cylindrical and
supersonic-area-rule designs although it is not correct to say this in a
strict sense.

The wings, of 5-percent-thick biconvex section, had a leading-edge
sweep of 45° and a taper ratio of 1.0. Wings 1 and 2 had aspect ratios
of 1.33 and 2.67, respectively; the dimensions are tabulated in figure 2.
An aspect ratio 2.67 wing-alone model, shown in figure 3, was also
constructed to check the wing-alone minimum wave-drag coefficient against
that predicted by linear theory. A wing-support model, which is that
part of the wing-alone model which fixes the wing in position, was tested
in order to determine its contribution to the measured drag of the
complete wing-alone model.

Procedure

Method of testing.- Force data were obtained from a three-component
electric strain-gage balance which measured normal force, chord force, and
pitching moment. Base-pressure measurements were obtained from photographic

recordings of a multiple-tube manometer using tetrabromethane as the measuring fluid. It was found necessary to use 10 to 12 orifices for measurement of the base pressure because the pressure field at the base of the models was not uniform. The orifice tubes leading from the models were mounted in a collar adjacent to the base of each model as shown in figure 4. The base-pressure collar was undercut 0.010 inch on its radius since this was the magnitude of the deflection of the model in its support system when at angle of attack. The angle-of-attack values were obtained from schlieren photographs taken of the model while the tunnel was running. Two horizontal wires were placed in one of the test-section windows to provide reference lines for use in measuring the angle of attack of the models. The photographs were then projected on the screen of an optical comparator and the angles of attack were measured with the aid of a large vernier protractor.

Testing conditions.- The models were tested at Mach numbers 1.39, 1.43, 1.75, and 1.97. The angle-of-attack range for the wing-body combinations was from 6° to -6° in increments of 1° or less. For the wing-alone studies, the angle-of-attack range was from 2° to -2° in increments of 1/2° or less. The Reynolds number was held at a constant value of approximately 1.5×10^6, based on the mean aerodynamic chord, throughout the Mach number range.

Boundary-layer transition was fixed by a 0.010-inch-diameter trip wire located 1 inch behind the apex of the nose cone and a 0.006-inch-diameter wire located 1/6th inch behind the leading edge of the wing. Reference 4 shows that under the conditions in which the boundary-layer trip wires were used in this test, the wires would cause transition of the boundary layer. For the wing-alone tests, no trip wires were used.

Uncertainty in Measurement

The uncertainty in Mach number was determined from the average deviation from the mean of several values as obtained from wind-tunnel total-pressure surveys over the region of the test section occupied by the models. The uncertainty in angle of attack was determined as the degree of repeatability in reading the angle of attack from schlieren photographs of the models. The uncertainties determined for the force coefficients were obtained from a statistical analysis which took into account the uncertainty in the balance forces, base pressures, and wind-tunnel stream characteristics. The uncertainty in the wing-alone and wing-support C_D was determined from the average deviation from the mean of the chord force coefficients through an angle-of-attack range from 2° to -2°.

The following table summarizes the uncertainties in measurement. The Mach numbers for the wing-body combinations are 1.39, 1.43, 1.75,

and 1.97. For the wing-alone and wing-support models, the Mach number is
1.43. The uncertainty in Mach number is ±0.005 and in angle of attack it
is ±0.05°.

Primary parameters		Uncertainty		
Configuration	α, deg	C_D	C_L	C_m
$B_1W_1, \ldots, B_5W_1$	0 ±6	±0.0007 ±.0021	±0.006	±0.01
$B_1W_2, \ldots, B_5W_2$	0 ±6	±.0012 ±.0028	±.007	±.02
Wing-alone	0	±.0004		
Wing support	0	±.0008		

RESULTS AND DISCUSSION

The results of the experimental tests are summarized in table II.
The information presented in the table is the minimum drag coefficient,
drag-rise factor, lift-curve slope, and pitching-moment-curve slope of
each configuration at various Mach numbers. The presentation of the data
in this manner is possible because the curves of ΔC_D vs. C_L^2, C_L vs. α,
and C_m vs. α were linear for the angle-of-attack range of the tests.
An examination of table II indicates that there is no systematic effect
of the body distortions on $\Delta C_D/C_L^2$, C_{L_α} and C_{m_α} of the wing-body
combinations. It should be pointed out that the tabulated values in
table II are the faired values of the data obtained experimentally and,
hence, are more accurate than the uncertainties in measurement which
were given previously.

Wing-Alone Results

The correct design of an optimum body distortion by the method of
quasi-cylindrical theory depends on the ability to predict the wing-alone
pressures and drag accurately. Since it is known that the pressure
distribution for a sonic-leading-edge wing cannot be accurately predicted,
a wing-alone model was tested to determine the inaccuracy in the predicted
wing-alone characteristics. The model was tested at a Mach number of 1.43
and the drag result was adjusted as subsequently explained to give the
minimum wave-drag coefficient. The experimental value of the minimum drag
coefficient of the model shown in figure 3 was 0.0163. The measured
$C_{D_{min}}$ of the wing support strut was 0.0045. The effect of the wing
support strut on the drag of the wing was estimated with the aid of
reference 5; the interference drag coefficient was found to be -0.0005.

Liquid film studies of the boundary-layer characteristics of the model placed the transition point at the wing midchord. By the use of the method of reference 6, the skin-friction drag coefficient was estimated to be 0.0040. Subtracting the support, interference, and skin-friction drag from the model drag gave a wing-alone minimum wave-drag coefficient of 0.0083 which is less than half the predicted value of 0.0188 obtained using the method of reference 7. This result is significant because it demonstrates that the wing-body combinations which were optimized according to theory would not give the predicted drag reductions experimentally. The reason for this can be seen by an examination of sketch (a) in the "Theoretical Considerations" section. The sketch shows that if the values of the points which define the curve of $C_{D_{W(d)}}$ are assumed too large, then the optimum point on the $\Delta C_{D_{min}}$ curve will be at a higher value of δ/a than it should be and, consequently, the greatest wave-drag reduction possible will not be realized experimentally.

Effects of Body Distortions at the Design Mach Number ($M_\infty = \sqrt{2}$)

The predicted and measured drag reductions obtained from the body distortions of quasi-cylindrical theory are shown in figures 5 and 6. The data points shown were obtained from the results summarized in tables II(a) and II(b). Figure 5 shows the results for the axisymmetric, n = 0, distortion. The figure shows that not only were drag reductions obtained experimentally for the design wing of A = 1.33, but even larger reductions were obtained for the A = 2.67 wing. This result may appear surprising at first; however, an explanation can be put forward which is consistent with the wing-alone results. It has been shown that linear theory overpredicts the pressures on a sonic-leading-edge wing and, therefore, the magnitude of the n = 0 body distortion (which was based upon the A = 1.33 wing pressures as computed by linear theory) is too large. Since the distortion required for an A = 2.67 wing is greater than that for an A = 1.33 wing, the distortion designed by theory for the smaller wing is more suitable for the large wing.

Figure 6 shows the additional reduction obtained by the application of one half of the nonaxisymmetric, n = 1, distortion. It was necessary to modify the n = 1 distortion because preliminary wind-tunnel tests indicated that adding the full n = 1 distortion increased the $C_{D_{min}}$ of the wing-body combination. A liquid-film study showed that the increase in $C_{D_{min}}$ was not caused by flow separation along the wing-body juncture. Therefore, testing of the n = 1 harmonic of distortion was discontinued because the linear-theory inadequacy for sonic-leading-edge wings apparently gave body distortions that were sufficiently large to exceed the drag-reducing range of δ/a on the $\Delta C_{D_{min}}$ curve of sketch (a). The experimental data in the figure show larger drag reductions for the A = 1.33 wing than for the A = 2.67 wing. This result is not in conflict

with the previous data since the n = 1 (modified) distortion apparently
agrees with the physically optimum distortion for the A = 1.33 wing
rather than for the A = 2.67 wing.

The experimental results shown in figures 5 and 6 indicate that drag
reductions are obtained from both the axisymmetric and nonaxisymmetric
distortions at the design Mach number of $\sqrt{2}$.

Effect of Mach Number

A comparison of the $M_\infty = 1.75$ and $M_\infty = 1.97$ data in figures 5 and 6
indicates that the drag reductions diminish slowly when departing from
the design condition. This would be expected from the discussion in the
"Theoretical Considerations" section. The figures also exhibit another
interesting result. At off-design Mach numbers, theory and experiment
are in better agreement than at the design Mach number. This effect is
also to be expected since the wing-alone pressures are more accurately
predicted for a supersonic leading edge than for a sonic leading edge.

Comparison Between the Supersonic Area Rule and Quasi-Cylindrical Theory

Figure 5 shows a comparison between the drag reductions obtained
from the supersonic area rule and the n = 0 distortion of the quasi-
cylindrical theory. The figure shows that the drag reductions for the
supersonic area rule are somewhat greater than those obtained by the
quasi-cylindrical theory for the particular case where the wing leading
edge is sonic at the design Mach number. The reader should be cautioned
that this comparison is not an indication of the over-all relative merits
of the two methods. Rather, it is a comparison only for the particular
case of a sonic-leading-edge wing for which linear theory is known to be
inaccurate.

CONCLUDING REMARKS

Axisymmetric and nonaxisymmetric body distortions designed by the
quasi-cylindrical theory of reference 2 and the supersonic area rule
without afterbody modification were tested to determine the amount of
wave-drag reduction obtainable over a Mach number range of 1.39 to 1.97.
Experimental results obtained from the tests show that both the axisym-
metric and nonaxisymmetric distortions yield drag reductions near the
design Mach number of $\sqrt{2}$. As would be expected, reductions diminish
with a departure from the design Mach number. No systematic effects of

the body distortions were noted on the drag-rise factors, lift-curve slopes, and pitching-moment curve slopes at zero lift.

Near the design Mach number, it was found that the quasi-cylindrical theory predicted a considerably larger drag reduction than was actually obtained. This was due to the fact that linear theory predicts too high a wave drag for a sonic-leading-edge wing and, correspondingly, optimum body distortions which are too great. For Mach numbers for which the wing leading edges were supersonic, the agreement between theory and experiment improved.

Near the design Mach number, and for the design aspect ratio of 1.33, the supersonic-area-rule distortion gave drag reductions comparable to those obtained by the quasi-cylindrical distortions. For the aspect ratio 2.67 configuration, the supersonic area rule gave somewhat greater reductions. The reader should be cautioned, however, that these comparisons are not indications of the over-all relative merits of the two methods. Rather, they are comparisons only for the particular case of a sonic-leading-edge wing for which linear theory is known to be inaccurate.

Ames Aeronautical Laboratory
    National Advisory Committee for Aeronautics
        Moffett Field, Calif., Sept. 18, 1956

REFERENCES

1. Jones, Robert T.: Theory of Wing-Body Drag at Supersonic Speeds.
    NACA RM A53H18a, 1953.

2. Nielsen, Jack N., and Pitts, William C.: General Theory of Wave-Drag
    Reduction for Combinations Employing Quasi-Cylindrical Bodies With
    an Application to Swept-Wing and Body Combinations. NACA TN 3722,
    1956. (Formerly NACA RM A55B07)

3. Lomax, Harvard, and Heaslet, Max. A.: A Special Method for Finding
    Body Distortions That Reduce the Wave Drag of Wing and Body Combi-
    nations at Supersonic Speeds. NACA RM A55B16, 1955.

4. Luther, Marvin: Fixing Boundary-Layer Transition on Supersonic-Wind-
    Tunnel Models. JPL Progress Report No. 20-256, Calif. Inst. of
    Tech., Jet Propulsion Lab., Aug. 12, 1955.

5. Jones, Robert T.: Properties of Low-Aspect-Ratio Pointed Wings at
    Speeds Below and Above the Speed of Sound. NACA TN 1032, 1946.

6. Vincenti, Walter G., Nielsen, Jack N., and Matteson, Frederick H.:
       Investigation of Wing Characteristics at a Mach Number of 1.53.
       I - Triangular Wings of Aspect Ratio 2. NACA RM A7I10, 1947.

7. Harmon, Sidney M., and Swanson, Margaret D.: Calculations of the
       Supersonic Wave Drag of Nonlifting Wings With Arbitrary Sweepback
       and Aspect Ratio - Wings Swept Behind the Mach Lines. NACA TN 1319,
       1947.

TABLE I.- FORMULAS AND CONDITIONS FOR COMPUTING BODY DISTORTIONS

$\frac{x}{a}$	Body 2 n = 0 $r_B = a(1 - \frac{t}{c}\lambda_0)$	Body 3 n = 0, 1(mod.) $r_B = a(1 - \frac{t}{c}\lambda_0 - \frac{1}{2}\frac{t}{c}\lambda_1 \cos 2\theta)$	Body 4 n = 0, 1 $r_B = a(1 - \frac{t}{c}\lambda_0 - \frac{t}{c}\lambda_1 \cos 2\theta)$	Body 5 supersonic area rule $r_B = a(1 - \frac{t}{c}\lambda)$
	λ_0	λ_1		λ
1.0	0	0		0
1.2	.203	.385		.044
1.4	.394	.887		.128
1.6	.580	1.457		.224
1.8	.754	2.074		.328
2.0	.914	2.728		.472
2.2	1.058	3.418		.528
2.4	1.176	4.100		.620
2.6	1.268	4.760		.696
2.8	1.326	5.346		.768
3.0	1.350	5.878		.820
3.2	1.340	6.276		.860
3.4	1.288	6.564		.880
3.6	1.199	6.714		.876
3.8	1.012 (1.052)[a]	6.682		.848
4.0	.657 (0.868)[a]	6.453		.792
	↓ Values of λ_0, λ_1, and λ are the same from $\frac{x}{a}$ of 4.0 to 8.0 ↓			↓
8.0	.657	6.453		.792

[a]Parentheses indicate correct values which were not used on the models.

TABLE II.- COMPILATION OF MINIMUM DRAG COEFFICIENT, DRAG-RISE FACTOR,
LIFT-CURVE SLOPE, AND PITCHING-MOMENT-CURVE SLOPE

Configuration	$C_{D_{min}}$ (1)	$\dfrac{\Delta C_D}{C_L{}^2}$	C_{L_α}	C_{m_α}	Configuration	$C_{D_{min}}$ (1)	$\dfrac{\Delta C_D}{C_L{}^2}$	C_{L_α}	C_{m_α}
(a) $M_\infty = 1.39$					(b) $M_\infty = 1.43$				
B_1W_1	0.0581	0.184	4.50	2.01	B_1W_1	0.0581	0.190	4.37	1.63
B_2W_1	.0574	.177	4.95	1.94	B_2W_1	.0578	.191	4.22	2.03
B_3W_1	.0554	.185	4.90	1.89	B_3W_1	.0555	.222	4.03	1.46
B_4W_1	.0601	.190	4.78	2.08	B_5W_1	.0570	.209	4.07	1.53
B_1W_2	.0410	.187	4.18	1.43	B_1W_2	.0410	.223	3.89	1.37
B_2W_2	.0386	.191	4.30	1.41	B_2W_2	.0390	.198	3.78	1.19
B_3W_2	.0377	.194	4.21	1.31	B_3W_2	.0380	.211	3.63	1.19
B_4W_2	.0397	.194	4.13	1.35	B_5W_2	.0370	.243	3.79	1.24
(c) $M_\infty = 1.75$					(d) $M_\infty = 1.97$				
B_1W_1	.0520	.219	4.01	1.50	B_1W_1	.0483	.212	4.16	1.40
B_2W_1	.0515	.211	4.60	1.46	B_2W_1	.0490	.220	4.22	1.31
B_3W_1	.0495	.250	3.77	1.48	B_3W_1	.0483	.240	4.06	1.73
B_5W_1	.0515	.153	4.51	1.48	B_5W_1	.0485	.220	4.20	1.42
B_1W_2	.0370	.246	3.34	1.15	B_1W_2	.0360	.256	3.62	1.10
B_2W_2	.0360	.216	3.29	1.15	B_2W_2	.0357	.261	3.42	---
B_3W_2	.0350	.275	3.02	1.10	B_3W_2	.0357	.264	3.63	1.15
B_5W_2	.0385	.218	3.60	1.05	B_5W_2	.0360	.232	3.44	.99

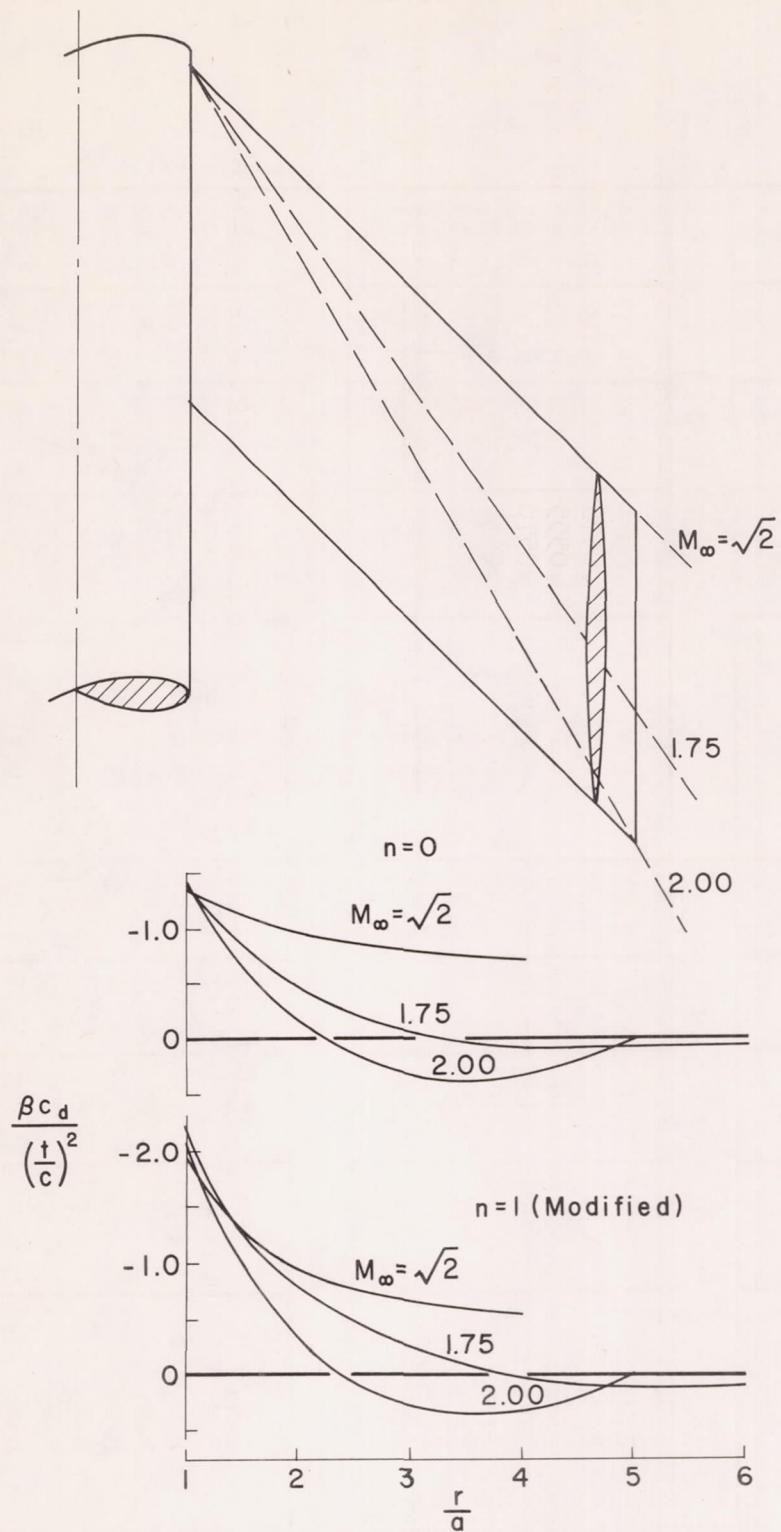[1]The values presented include turbulent skin friction, transition wire, and wave drag and are presented for comparison purposes only.

Figure 1.- Spanwise variation of the theoretical section drag
coefficient due to body distortions.
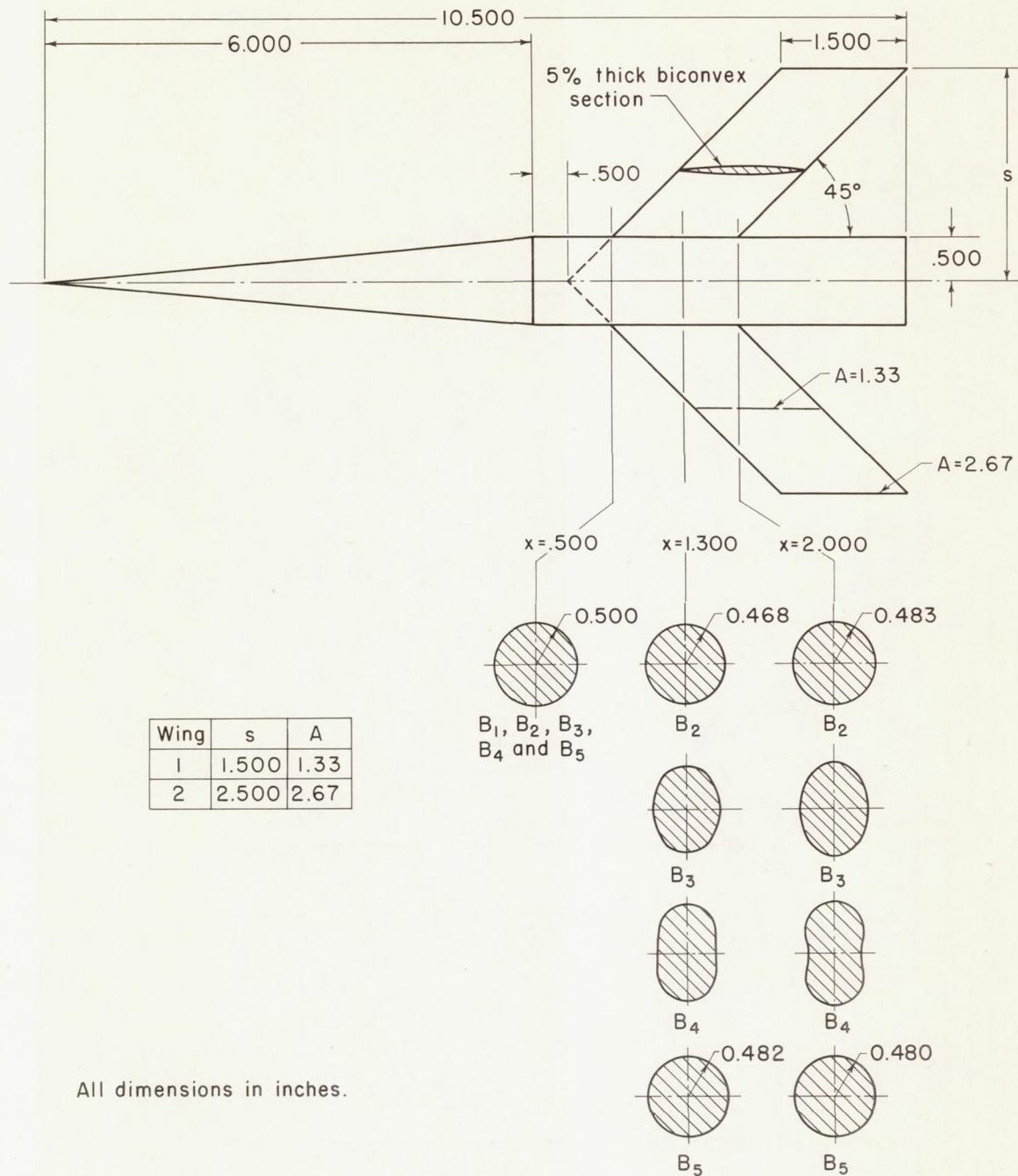
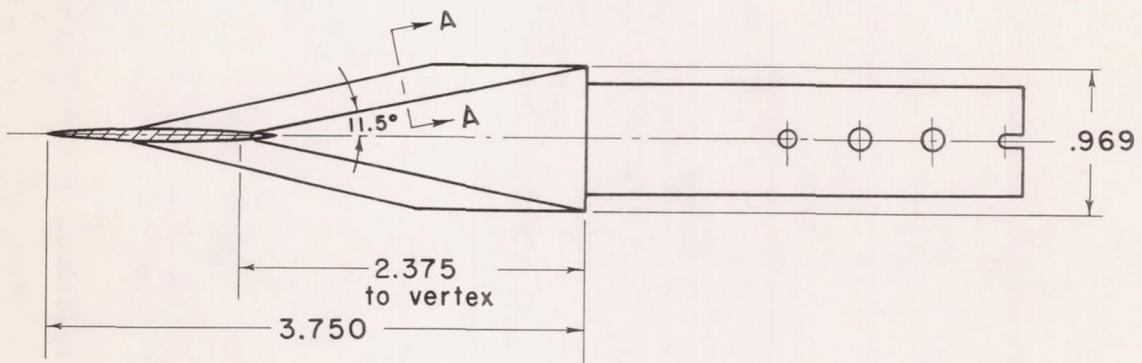Figure 2.- Plan-form dimensions and section views of models.

1.500

45°

.125

.172

2.000

All dimensions in inches.

18°

Section A-A

A

11.5°

A

.969

2.375
to vertex

3.750
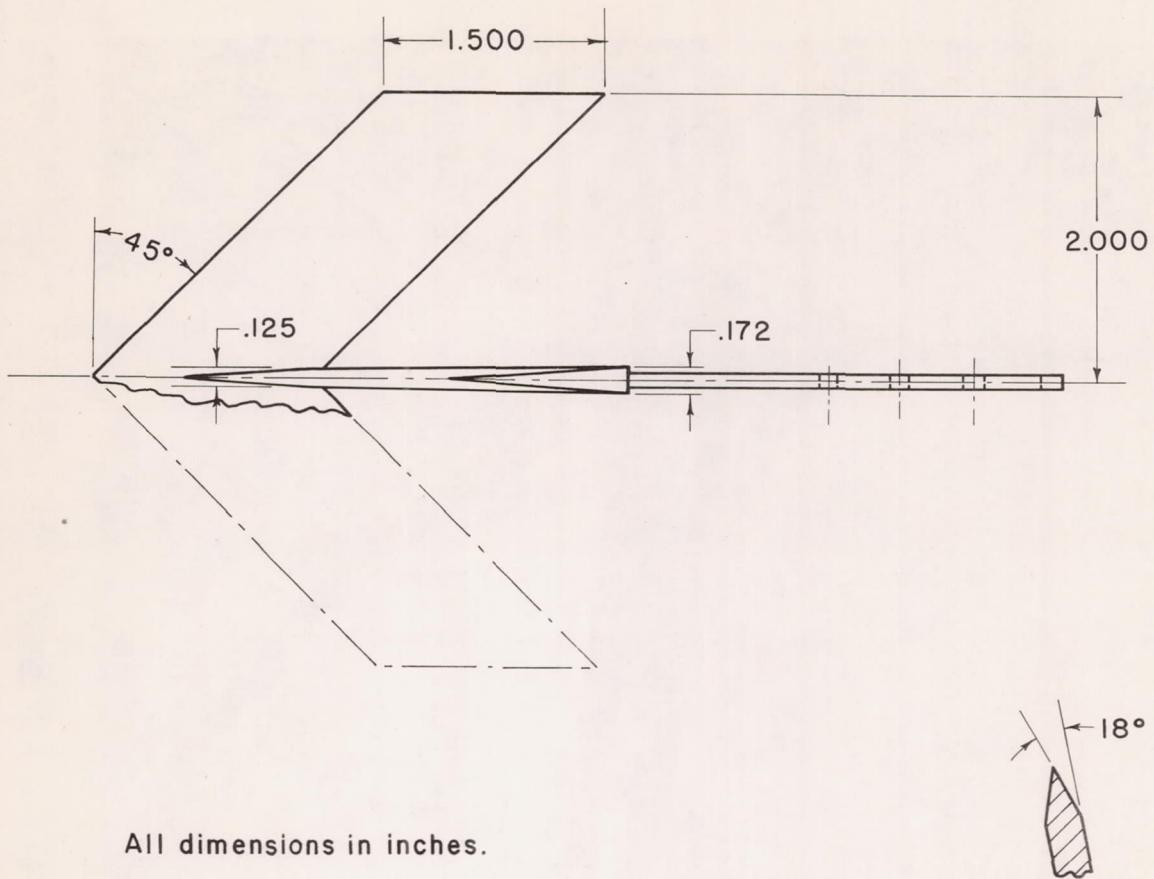
Figure 3.- Wing-alone model.
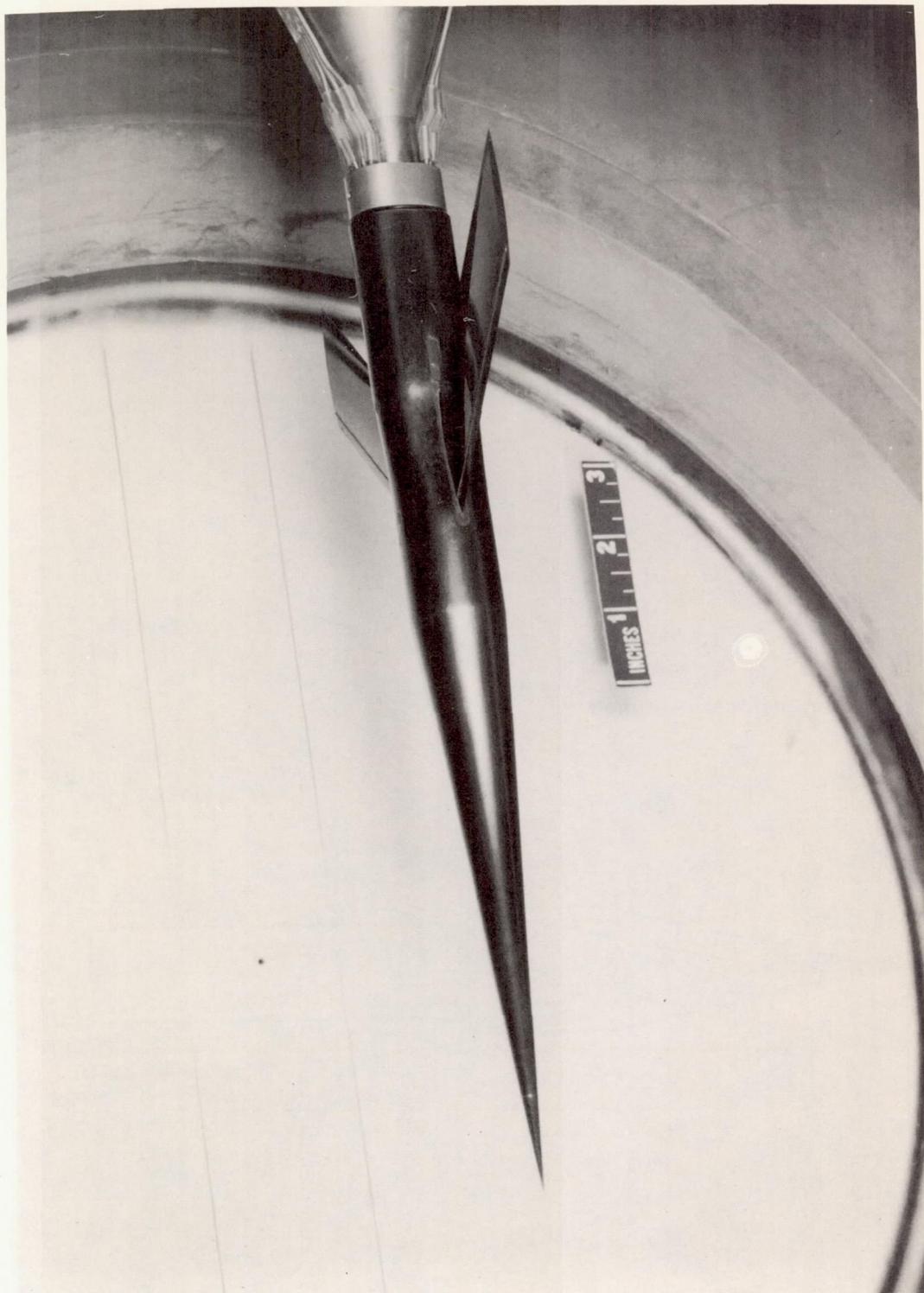
Figure 4.- Tunnel installation of configuration B_3W_2.

A-20424

CONFIDENTIAL   19

Quasi-cylindrical theory (ref. 2)

n=0 distortion

$\odot \left(\Delta C_{D_{min}} = C_{D_{min_{B_2 W_1}}} - C_{D_{min_{B_1 W_1}}}, \right.$
$\left. C_{D_{min_{B_2 W_2}}} - C_{D_{min_{B_1 W_2}}} \right)$

Supersonic area rule

$\triangle \left(\Delta C_{D_{min}} = C_{D_{min_{B_5 W_1}}} - C_{D_{min_{B_1 W_1}}}, \right.$
$\left. C_{D_{min_{B_5 W_2}}} - C_{D_{min_{B_1 W_2}}} \right)$

$\Delta C_{D_{min}}$

$W_1, A = 1.33$

$\Delta C_{D_{min}}$

$W_2, A = 2.67$

M_∞
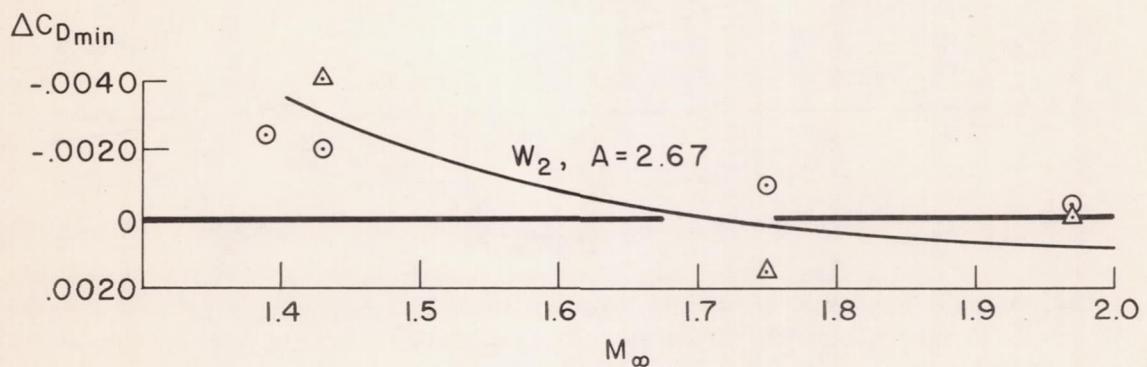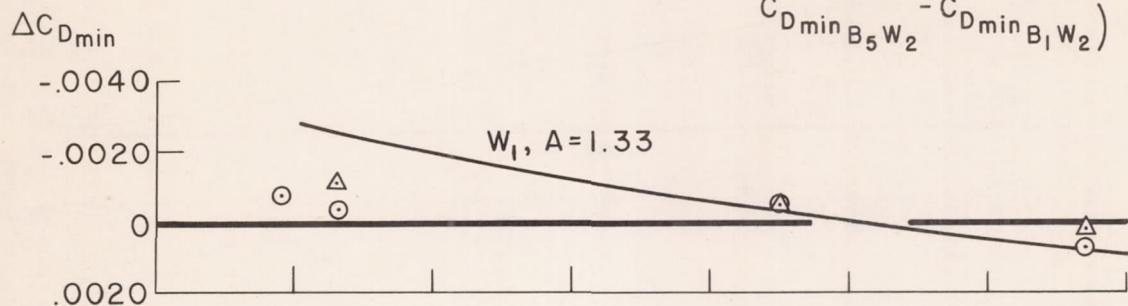
Figure 5.- Comparison of the theoretical and experimental drag
reductions for the axisymmetric distortions.

Quasi-cylindrical theory (ref. 2)

n = 1 (modified) distortion
$$\left(\Delta C_{D_{min}} = C_{D_{min}B_3 W_1} - C_{D_{min}B_2 W_1}, \quad C_{D_{min}B_3 W_2} - C_{D_{min}B_2 W_2} \right)$$

$\Delta C_{D_{min}}$

W_1, A = 1.33

$\Delta C_{D_{min}}$

W_2, A = 2.67

M_∞
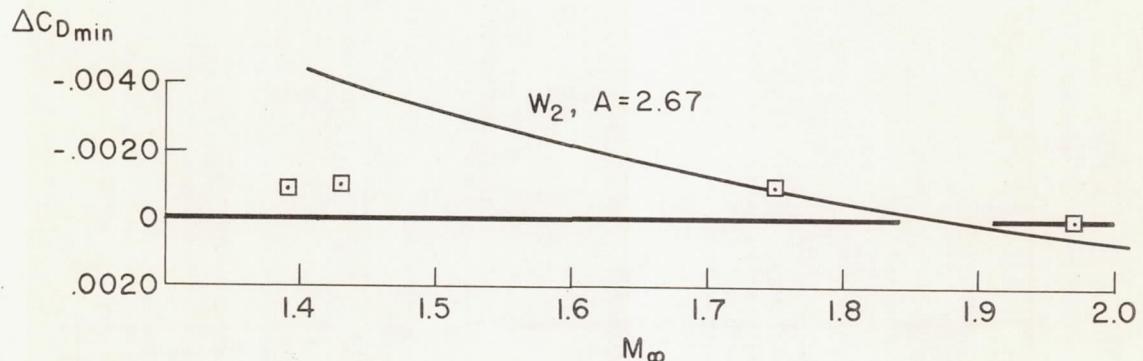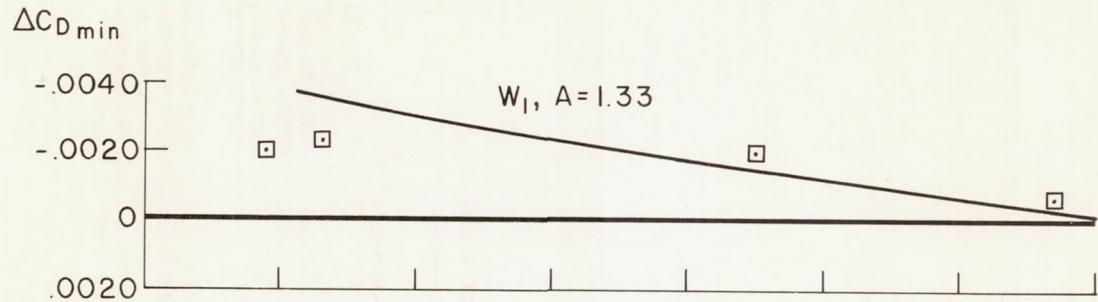
Figure 6.- Comparison of the theoretical and experimental drag reductions for the n = 1 (modified) distortion.